

PREPARED FOR SUBMISSION TO JHEP

QGP time formation in holographic shock waves model of heavy ion collisions¹

Irina Ya. Aref'eva

*Steklov Mathematical Institute, Russian Academy of Sciences,
Gubkina str. 8, 119991, Moscow, Russia*

E-mail: arefeva@mi.ras.ru

ABSTRACT: We estimate the thermalization time in two colliding shock waves holographic model of heavy-ion collisions. For this purpose we model the process by the Vaidya metric with a horizon defined by the trapped surface location. We consider two bottom-up AdS/QCD models that give, within the colliding shock waves approach, the dependence of multiplicity on the energy compatible with RHIC and LHC results. One model is a bottom-up AdS/QCD confining model and the other is related to an anisotropic thermalization. We estimate the thermalization time and show that increasing the confining potential decreases the thermalization time as well as an anisotropy accelerates the thermalization.

KEYWORDS: Quark gluon plasma, heavy-ion collisions, thermalization, AdS/CFT correspondence, holography, Lifshitz-like metric

¹Based on invited talks at International Conference on "Quark Confinement and the Hadron Spectrum XI" (confinement XI), St. Petersburg, Russia, 7-13 Sep. 2014 and International Conference on Physics "In Search of Fundamental Symmetries" dedicated to the 90-th birthday anniversary of Yu.V. Novozhilov, 1-5 Dec. 2014.

Contents

1	Introduction	2
2	Thermalization in isotropic backgrounds	4
2.1	Setup	4
2.1.1	General isotropic metric	4
2.1.2	Thermalization due to shock waves collision	4
2.2	Thermalization Times	7
2.2.1	Estimation with the Vaidya metric	7
2.2.2	Estimation for confining metric	8
2.2.3	Estimation for power metric	10
2.2.4	Estimation of the formation time of a trapped surface by non-local correlation functions	13
3	Thermalization in anisotropic backgrounds	14
3.1	Setup	14
3.1.1	Anisotropic metrics	14
3.1.2	Thermalization due to shock waves collision	15
3.2	Thermalization time in the anisotropic background	16
3.2.1	Estimation with Vaidya metric	16
3.2.2	Estimation with non-local correlation functions	16
4	Conclusion	19

1 Introduction

Holographic duality [1–3] provides a powerful tool for studying static properties of the QGP as well as its thermalization [4–6]. There are holographic models that reproduce perfectly the static properties of the QGP, meanwhile others holographic models are used to get non-static characteristics such as the thermalization time in heavy-ion collisions and the charged multiplicity. Holographic thermalization means a black hole formation in the dual space-time and particle multiplicities is defined by the entropy of the produced black hole.

The gauge/string duality [1–3] perfectly works for the $\mathcal{N}=4$ Supersymmetric Yang-Mills theory, while a true dual description of real QCD is unknown, in spite of a lot of efforts have been made to find holographic QCD from string setup [7–13]. This approach is known as the ”top-down” approach. Other approach, known as the ”bottom-up” approach, is supposed to propose a holographic QCD model, i.e. a suitable vacuum background, that fits experimental data and lattice results. The quark confining backgrounds that reproduce the Cornell potential, ρ -meson spectrum etc. have been proposed in [14–19]. Improved holographic QCD (IHQCD) that reproduce the QCD β -function have been proposed in [20, 21]. The dual holographic approach has been successfully used to describe the static properties of the QGP, see [4] for review.

The problem of the QGP formation in HIC is the subject of intensive study within the holographic approach in last years (see reviews [5, 6, 22] and refs therein) and initially has been considered in the AdS background [23]–[31], that cannot describe either quark confinement either reproduce the QCD β -function. However, as we have just mentioned, there are backgrounds which solve one, or even two of these problems. Therefore, to describe the holographic thermalization in more realistic frameworks, it is natural to study thermalization in these backgrounds.

Thermalization in the improved holographic background has been studied in [32] and it has been shown that without additional assumptions, such as an energy dependent cut-off at the high energy [28], one cannot reproduce the multiplicity dependence on energy observed at RHIC and LHC in this background. In [33] it has been noticed that the holographic realization of the experimental dependence of multiplicity on the energy [35] requires an unstable background. In [36] it has been shown that the model reproducing the Cornell potential also gives an observed energy dependence of multiplicities if one assumes that the multiplicity is related to the dual entropy produced during a limited time period. However in this consideration there is a limitation on the possible energy of colliding shock walls [36]. Since in this consideration we have used a more or less general background reproducing AdS at UV and confinement at IR, we can think that just general assumptions about the background prevent to reproduce suit-

able behavior in UV and IR and in the same time give the correct energy dependence of multiplicity at *high energy*. In particular, we can think that a default assumption of the isotropic form of background metrics is responsible for this discrepancy and for a more realistic description of entropy production in holographic models one has to consider anisotropic backgrounds [38].

In favor of anisotropic holographic backgrounds there are also additional arguments (see review [39] for holographic studies of strong coupled anisotropic theories). Up to a year ago, it was believed that just after heavy-ion collisions, a pre-equilibrium period exists for up to 1 fm/c and then the QGP appears and this QGP is isotropic. However now there is a belief that the QGP is created after a very short time after the collision, $\tau_{therm} \sim 0.1 fm/c$, and it is anisotropic ("anisotropic" means to a spatially anisotropy) for a short time τ after the collision, $0 < \tau_{therm} < \tau < \tau_{iso}$, and the time of locally isotropization is about $\tau_{iso} \sim 2 fm/c$ [37]. In the holographic version of this setup it is suitable to consider a black hole formation in a spatially anisotropic background. Motivated by recent experimental indications in favor of anisotropic thermalization, we also discuss a holographic thermalization scenario in the anisotropic 5-dimensional Lifshitz-like background. The collision of domain walls in this background has been recently considered in [38], where it has been shown that for the critical exponent specifying the Lifshitz-like background equal to 4, the dependence of multiplicity on the energy is desirable $E^{1/3}$.

In this paper we estimate thermalization time for two colliding shock waves in different backgrounds. Our main idea is very simple – the black hole creation in two shock waves collisions is modeled by Vaidya metric with a horizon corresponding to the location of the trapped surface appearing in two shock waves collision and thermalization time is estimated within standard prescription in the Vaidya metric [41]. The Vaidya deformation of isotropic backgrounds have been successfully used in description of thermalization in several isotropic models [41]–[50] as well as Vaidya deformations [51–54] of anisotropic metrics [56, 58–63].

As mentioned above, only for a special background the entropy of the black hole produced in the domain shock wave collision reproduces the energy dependence of particle multiplicities obtained at RHIC and LHC. We estimate the thermalization time for these cases. Namely, we estimate the isotropic/anisotropic thermalization time in a holographic bottom-up AdS/QCD confinement background that provides the Cornell potential and QCD β -function. Here we use the Vaidya deformation of confinement background metrics in both isotropic and anisotropic cases. We also compare these results with our previous results obtained by general causality arguments [36]

The paper is organized as follows. In Section 2 we discuss the isotropic case and in Section 3 the anisotropic one. Both sections are started by setup, where notations

and review of previous results are presented. In main parts of the sections estimations of thermalization time by the Vaidya modeling are performed. A comparison of results obtained by Vaidya modeling and by general causal arguments are presented in the end of these sections.

2 Thermalization in isotropic backgrounds

2.1 Setup

2.1.1 General isotropic metric

In a general isotropic holographic approach, the 5-dimensional metric is

$$ds^2 = b^2(z)(-dt^2 + dz^2 + dx_i^2), \quad i = 1, 2, 3. \quad (2.1)$$

Following [32] we consider the following form of the b-factor

$$b(z) = \frac{e^{cz^2/4}}{z^a}, \quad (2.2)$$

where a and c are some constants. Metric (2.1) in the top-down approach supposes to solve the 5-dimensional dilaton-gravity equations of motion [20, 21]. It is also considered in the bottom-up approach, in particular, the confining metric considered in [14] corresponds to $a = 1$ and $c = 0.42 \text{ GeV}^2$, see also [16–19].

2.1.2 Thermalization due to shock waves collision

Point-like shock waves are usually considered in top-down backgrounds and they are supposed to be solutions of the 5-dimensional (dilaton) gravity with point-like sources. In the case of the point-like shock wave the deformation of metric (2.1) has the form

$$\begin{aligned} ds_{shock}^2 &= ds^2 + \delta ds_{shock}^2, \\ \delta ds_{shock}^2 &= b^2(z) \phi(z, x_1, x_2) \delta(u) du^2. \end{aligned} \quad (2.3)$$

Here and below $u, v = t \pm x_3$ and the point shock profile $\phi(z, x_1, x_2)$ solves the equation

$$\square_{3b} \phi(z, x_1, x_2) = -16\pi G_5 J_{uu}, \quad \square_{3b} = (\partial_\alpha \partial_\alpha + 3 \frac{\partial_z b}{b} + \partial_z^2), \quad (2.4)$$

here \square_{3b} is the Beltrami-Laplace operator corresponding to metric $ds_{3b}^2 = b^2(z)(dz^2 + dx_\perp^2)$, $\perp = 1, 2$, G_5 is the 5-dimensional gravitational constant and J_{uu} is the component of the energy-momentum tensor sourcing the point-like shock wave, $J_{uu} \sim \delta(u) \delta(z - L) \delta(x_\perp)$.

Two colliding point-like shock waves

$$\delta ds_{2-shocks}^2 = b^2(z) (\phi(z, x_1, x_2) \delta(u) du^2 + \phi(z, x_1, x_2) \delta(v) dv^2), \quad u, v < 0, \quad (2.5)$$

produce a black hole, whose entropy \mathcal{S} can be estimated by the area of the trapped surface

$$\mathcal{S} \geq \mathcal{S}_{TS}, \quad \mathcal{S}_{TS} = \frac{2}{4G_5} \int_{z_a}^{z_b} \sqrt{\det |g_{3b}|} dz dx_\perp^2 = \frac{\pi}{2G_5} \int_{z_a}^{z_b} b(z)^3 x_\perp^2(z) dz. \quad (2.6)$$

z_a and z_b are the points where $\psi(z_{a,b}) = 0$. $\psi(z)$ is the trapped surface profile function, which for the central collision [24, 32] up to the boundary conditions (that in fact define $z_{a,b}$) satisfies the same equation as the shock wave profile.

The simplest form of the black hole in the background metric (2.1) is given by [20]

$$ds^2 = b^2(z) (-f(z_h, z) dt^2 + \frac{dz^2}{f(z_h, z) z^2} + dx_i^2), \quad i = 1, 2, 3, \quad (2.7)$$

$$f(z_h, z) = 1 - K(z_h, z), \quad K(z_h, z) = \frac{K(z)}{K(z_h)}, \quad (2.8)$$

$$K(z) = \int_0^z \frac{dz}{b(z)^3}, \quad (2.9)$$

here z_h is the position of the horizon, and the temperature and entropy are

$$\frac{1}{T} = \frac{4\pi}{f'(z_h)} = 4\pi \int_0^{z_h} \frac{b(z_h)^3}{b(z)^3} dz, \quad (2.10)$$

$$\mathcal{S}_f = \frac{b^3(z_h) \mathcal{V}_3}{4G_5}, \quad (2.11)$$

where \mathcal{V}_3 is the volume of the 3-dim space.

For the *shock domain walls* [30, 31] the wave profile does not depend on the transversal coordinates and solves

$$\left(\partial_z^2 + \frac{3b'}{b} \partial_z \right) \phi^w(z) = -\frac{16\pi G_5 E}{L^2} \frac{\delta(z - z_*)}{b^3(z)}. \quad (2.12)$$

The trapped surface is located between points z_a and z_b which satisfy equations [33]

$$\begin{aligned} \frac{8\pi G_5 E}{L^2} b^{-3}(z_a) \int_{z_b}^{z_*} b^{-3} dz &= \int_{z_b}^{z_a} b^{-3} dz, \\ \frac{8\pi G_5 E}{L^2} b^{-3}(z_b) \int_{z_a}^{z_*} b^{-3} dz &= - \int_{z_b}^{z_a} b^{-3} dz, \end{aligned} \quad (2.13)$$

here z_* is the position of the collision point. The area density s (per the area in the transversal direction) of the trapped surface located between points z_a and z_b , is given by

$$s = \frac{1}{2G_5} \int_{z_a}^{z_b} b^3 dz. \quad (2.14)$$

Equations (2.13) give the relation between points z_b , z_a and the energy E ,

$$b^3(z_a) + b^3(z_b) = \frac{8\pi G_5 E}{L^2}. \quad (2.15)$$

2.2 Thermalization Times

2.2.1 Estimation with the Vaidya metric

In this section we model the black hole creation in two shock waves collision by the Vaidya metric with a horizon corresponding to the location of the trapped surface appearing in these shock waves collision and estimate the thermalization time within the standard prescription in the Vaidya metric [41].

We relate z_a and z_b , defining the location of the trapped surface, with the masses M_a and M_b of the black brane in the background (2.1),

$$M_a \equiv M(z_a), \quad M(z_a) = K^{-1}(z_a), \quad (2.16)$$

where $K(z)$ is defined by (2.9), and the same for z_b . We assume that from $z_a < z_b$ it follows that $M_b < M_a$. The appearance of the trapped surface located at z_a and $z_b = \infty$ can be modeled by the Vaidya metric

$$ds^2 = b^2(z) \left(-f(z_h, z, v) dv^2 - 2dv dz + d\vec{x}^2 \right), \quad (2.17)$$

$$f(z_a, z, v) = 1 - \theta(v) K(z_a, z). \quad (2.18)$$

As it is accepted in the Vaidya approach [41]-[50], to find the thermalization time τ at the scale ℓ one has to consider a geodesic with equal time endpoints located at the boundary at distance ℓ and find the time τ , when this geodesic is covered by the black shell (2.17). The thermalization time τ and the distance ℓ are related as

$$\ell = 2s \int_0^1 \frac{b(s)}{b(sw)} \frac{dw}{\sqrt{(1 - K(z_h, sw)) \cdot \left(1 - \frac{b^2(s)}{b^2(sw)}\right)}}; \quad (2.19)$$

$$\tau = s \int_0^1 \frac{dw}{1 - K(z_h, sw)}, \quad (2.20)$$

i.e. one finds the thermalization time at the scale l excluding the axillary parameter s from the system of equations (2.19) and (2.20),

$$\tau = \tau_{therm}(z_h, l). \quad (2.21)$$

Assuming $z_a < z_b$ we estimate the thermalization time due to the trapped surface formation by

$$\tau_{therm}(z_a, z_b, l) = \tau_{therm}(z_a, l). \quad (2.22)$$

2.2.2 Estimation for confining metric

In this section we consider thermalization for the metric with the confining b -factor

$$b(z) = \frac{e^{cz^2}}{z}, \quad (2.23)$$

here c is related with the notations of [15] as $c = \frac{1}{4}c_{AZ}$ and we use the bottom-up version of the blackening function considered in [14]

$$K(z) = z^4, \quad f(z_h, z) = 1 - \frac{z^4}{z_h^4}. \quad (2.24)$$

Note that according (2.16) there are non-leading corrections to (2.24). Indeed, for the b -factor (2.23) the blackening function according (2.16) is

$$K(z_a, z) = \int_0^{z_a} \frac{dz}{b(z)^3} = \frac{-1 + e^{-3cz^2} + 3e^{-3cz^2}cz^2}{-1 + e^{-3cz_h^2} + 3e^{-3cz_h^2}cz_h^2}. \quad (2.25)$$

The leading term is in agreement with (2.24)

$$K(z_a, z) = k_4 z^4 + k_6 z^6 + \mathcal{O}(z^8), \quad (2.26)$$

where $k_4 = 1/z_h^4 + 2c/z_h^2 + \mathcal{O}(1)$, $k_6 = -2c/z_h^4 + \mathcal{O}(1)$.

In Fig.1.A the dependence of the thermalization time τ on the scale ℓ for the metric (2.23) for different values of c is shown. From this plot we see that increasing the confinement potential, in fact when c in formula (2.23) increases, we decrease the thermalization time.

In Fig.1.B. the dependence of $v = \ell/\tau$ on l for the same parameters as in Fig.1.A is presented. We can interpret $v = l/t$ as a propagation velocity of the thermalization. We see that the velocity increases with increasing of the factor c in (2.23).

In Fig.2.A. dependencies of τ on ℓ for different masses of the shell and the same parameters c as in Fig.1.A are presented. We see that for chosen parameters the dependence on z_h is very small. We see that increasing z_h for AdS case we increase the thermalization time. The same is true for $c = 0.1$. However, when we increase c so that $0.2 < c < 0.5$ the dependence on z_h becomes more essential (the distances between the magenta lines are larger as compared with distances of green lines) and when increasing z_h we decrease the thermalization time. We also see, Fig.2.B., that in considered cases only up to some given distance the thermalization is possible. This is related with the breaking of geodesics with two large endpoints distance in the confining background.

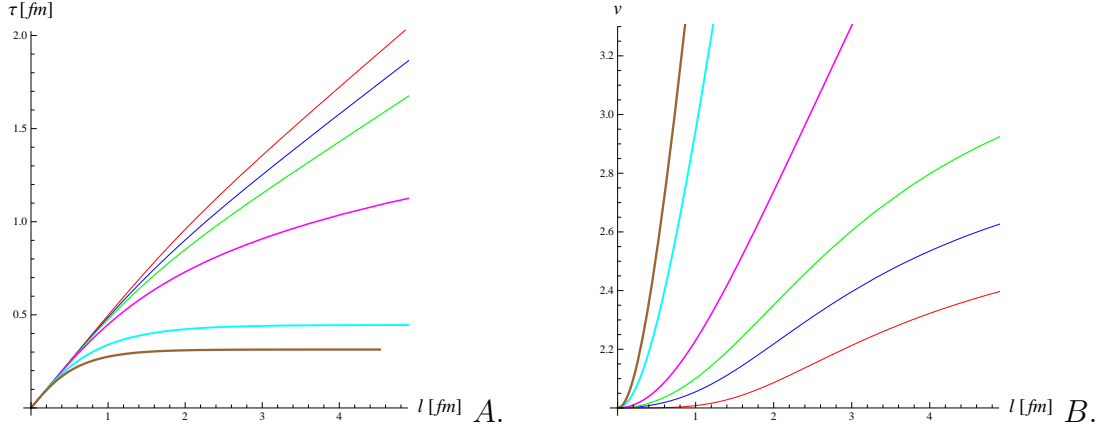


Figure 1. A. Dependencies of τ on ℓ for 5-dimensional metric (2.17) with the confining b -factor (2.23) for $c = 0$ (red), $c = 0.1$ (blue), $c = 0.2$ (green), $c = 0.5$ (magenta), $c = 2.56$ (cyan), $c = 5.16$ (brown) and the blackening factor (2.16) with $z_h = 1$. B. Dependencies of $v = \ell/\tau$ on ℓ for the same parameters as in the left panel.

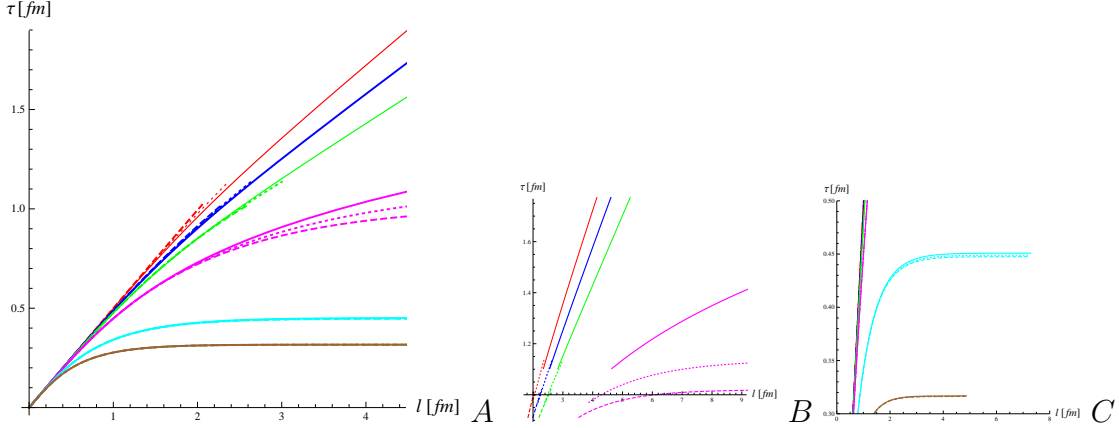


Figure 2. A. Dependencies of τ on ℓ for the 5-dimensional metric (2.17) with the confining b -factor (2.23) for $c = 0$ (red), $c = 0.1 \text{ fm}^{-2}$ (blue), $c = 0.2 \text{ fm}^{-2}$ (green), $c = 0.5 \text{ fm}^{-2}$ (magenta), $c = 2.56 \text{ fm}^{-2}$ (cyan), $c = 5.16 \text{ fm}^{-2}$ (brown) and $z_h = 1 \text{ fm}$ (solid lines), $z_h = 1.2 \text{ fm}$ (dotted lines), $z_h = 1.8 \text{ fm}$ (dashed lines). B. The zoom of the plot A in the region $2 \text{ fm} < \ell < 9 \text{ fm}$ and $1 \text{ fm} < \tau < 1.8 \text{ fm}$. C. The zoom of the plot A in the region $0 < \ell < 8 \text{ fm}$ and $0.3 \text{ fm} < \tau < 0.5 \text{ fm}$.

In Fig. 3 the thermalization process is presented for more realistic values of c , namely $c = 2.56 \text{ fm}^{-2}$. Dependencies of τ on ℓ for 5-dimensional metric (2.17) with the confining b -factor (2.23) with $c = 2.56$ and different blackening functions: blackening function (2.28) for $z_h = 1.2$ and $z_h = 1.8$ corresponds to solid and dashed blue lines; blackening

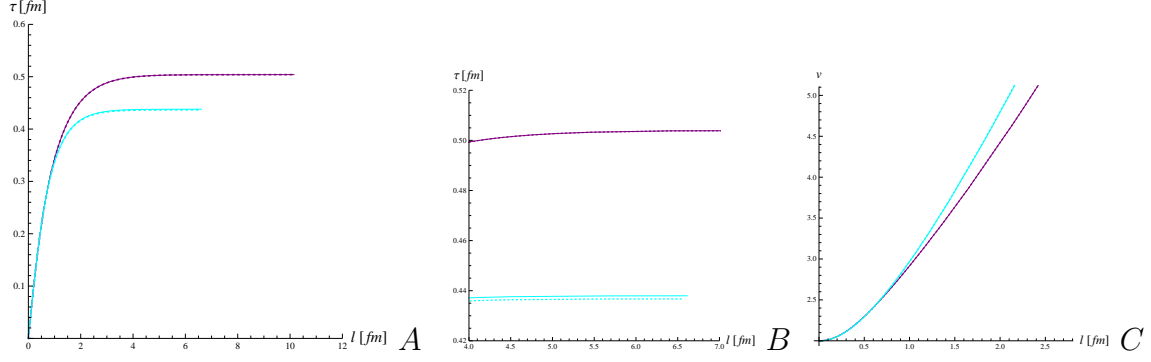


Figure 3. A. Dependencies of τ on ℓ for the 5-dimensional metric (2.17) with the confining b -factor (2.23) with $c = 2.56$ and different blackening functions: blackening function (2.28) for $z_h = 1.2$ and $z_h = 1.8$ corresponds to solid and dashed blue lines; blackening function (2.25) for $z_h = 1.2$ and $z_h = 1.8$ corresponds to solid and dashed red lines. B. The zoom of the plot A. C. Dependencies of τ/ℓ on ℓ for the same parameters as in the plot A.

function (2.25) for $z_h = 1.2$ and $z_h = 1.8$ corresponds to solid and dashed red lines. We see that corrections (2.26) do not play an essential role for small distances, but at large distances the blackening factor (2.24) admits longer geodesics as compared with (2.25).

2.2.3 Estimation for power metric

It is instructive to compare estimations obtained in the previous subsection 2.2.2 with results obtained for the intermediate metric [36]

$$ds_{inter}^2 = \left(\frac{L_{eff}}{z} \right)^{2a} (-dt^2 + dz^2 + dx^2), \quad (2.27)$$

In this case the blackening function is

$$f(z) = 1 - \frac{z^{da+1}}{z_h^{da+1}}, \quad (2.28)$$

and the thermalization time τ at the scale l is

$$\ell = 2s \int_0^1 \frac{w^a dw}{\sqrt{\left(1 - \frac{s^{1+da}}{z_h^{1+da}} w^{1+da}\right) (1 - w^{2a})}}, \quad (2.29)$$

$$\tau = s \int_0^1 \frac{dw}{\left(1 - \frac{s^{1+da}}{z_h^{1+da}} w^{1+da}\right)}. \quad (2.30)$$

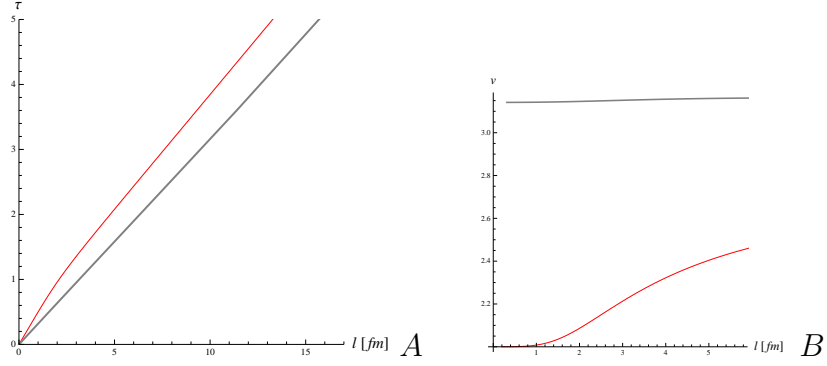


Figure 4. A. Dependencies of τ on ℓ for 5-dimensional metric (2.17) with the power-law b -factor (2.27) for $a = 1$ (solid red line), i.e. the AdS_5 case and $a = 0.5$ (thick gray line). B. Velocities for the same parameters.

In Fig.4.A dependencies of τ on ℓ for 5-dimensional metric (2.17) with the power b -factors (2.27): $a = 1$ (solid line), i.e. the AdS_5 case, and $a = 0.5$ (dashed line) are presented. We see that decreasing a we decrease the thermalization time. From Fig.4 we see that the velocity of propagation of thermalization increases with decreasing a .

It is interesting to note that the dependence of t on l does not depend on the position of the horizon for $a = 1$, i.e.

$$\tau(z_h, l)|_{a=1} = \tau(1, l)|_{a=1} \quad (2.31)$$

The confirmation of (2.31) is presented in Fig.5. Indeed, we see in the plots in Fig.5 that three lines, the purple thick line, the red solid line and the dashed blue one coincide, i.e. the thermalization time does not depend on z_h .

From (2.29) and (2.30) it is evident that

$$\frac{\ell}{z_h} = 2S \int_0^1 \frac{w^a dw}{\sqrt{(1 - S^{1+da} w^{1+da})(1 - w^{2a})}}, \quad (2.32)$$

$$\frac{\tau}{z_h} = S \int_0^1 \frac{dw}{(1 - S^{1+da} w^{1+da})}, \quad (2.33)$$

here we introduce a new parameter $S = s/z_h$. The system of equations (2.32) and (2.33) is nothing but the system of equations that defines the thermalization time in units of z_h for the Vaidya model with the unique mass, i.e.

$$\tau = z_h \tau_{therm}\left(1, \frac{\ell}{z_h}\right). \quad (2.34)$$

Note that in [36] we have shown that the b -factor for the intermediate metric (2.27) with $a = 0.5$ and $L_{eff} = 20.86$ approximates the confining b -factor for $1.2 fm <$

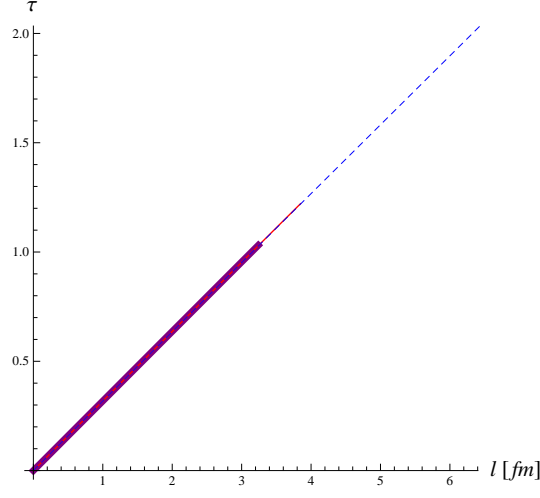


Figure 5. A. Dependencies of τ on ℓ for 5-dimensional metric (2.17) with the power b -factor (2.27) for $a = 0.5$ and blackening factor (2.28) with different z_h : $z_h = 1$ (blue dashed line), $z_h = 1.5$ (red solid line), $z_h = 2.5$ (purple thick solid line).

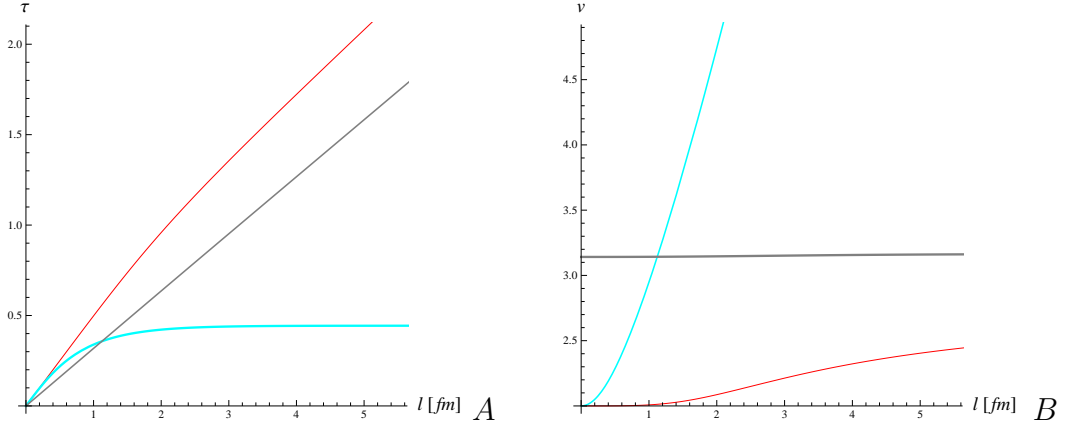


Figure 6. A. Dependencies of τ on ℓ for 5-dimensional metric (2.17) with different b -factors: the thin red line corresponds to power factor (2.27) with $a = 1$ (AdS); the gray line corresponds to $a = 0.5$ and the thick cyan line corresponds to the factor (2.23) with $c = 2.56$. B. Dependencies of velocities of the propagation of thermalization on the characteristic distance.

$z < 1.8 fm$. For $z \sim 1.1 fm$ the thermalization times for these two models are very close, however, for the distance $z \sim 2 fm$ thermalization times are different up to factor 0.3. For larger distances these two models show essentially different behaviour: the thermalization time for the confining metric does not depend essentially on the distances, meanwhile the intermediate model has approximately a linear dependence of the thermalization time on the distance.

In Fig.6. A. we plot the dependence of the thermalization time for 3 different models: the AdS case (thin solid red line), the intermediate case [36] (gray line) and for the confining factor [14] (thick cyan line). For all cases $z_h = 1 \text{ fm}$.

The small dependence of the thermalization time on the value of the mass of the shell for special models can be seen from the following considerations. Assuming that $b(z)$ satisfies the scaling

$$b(kz) = k^{s_b} b(z) + \dots, \quad 0 < z < z_h, \quad (2.35)$$

one can reduce the problem of finding the thermalization time at the scale ℓ by the Vaidya metric with mass M_h to the same problem with the unite mass. Indeed, from (2.35) and (2.16) the scaling for the mass $M(z)$ is

$$M^{-1}\left(\frac{z}{k}\right) \approx k^{d_{s_b}-1} M^{-1}(z). \quad (2.36)$$

Performing the rescaling

$$z = k_a \tilde{z}, \quad x = k_a \tilde{x}, \quad t = k_a \tilde{t}, \quad (2.37)$$

with

$$k_a = M_a^{\frac{1}{d_{s_b}-1}} \quad (2.38)$$

we recast the metric (2.17) to the same form in terms of the tilde-coordinates and the blackening function with a unit mass $f(1, \tilde{z}, \tilde{v})$,

$$ds^2 = M_a^{\frac{2s_b+2}{d_{s_b}-1}} b^2(\tilde{z}) \left(-f(1, \tilde{z}, \tilde{v}) d\tilde{v}^2 - 2d\tilde{v}d\tilde{z} + d\vec{\tilde{x}}^2 \right). \quad (2.39)$$

Therefore,

$$\tau_{therm}(z_a, l) = k_a \tilde{\tau}_{therm}(1, \tilde{\ell}) = k_a \tau_{therm}(1, \ell/k_a). \quad (2.40)$$

Assuming that

$$\tau_{therm}(1, \ell) = C_1 \ell + C_2 \ell^2 + \dots \quad (2.41)$$

we get

$$\tau_{therm}(z_a, z_b, \ell) \approx C_1 + C_2 \ell^2 / k_a^2. \quad (2.42)$$

2.2.4 Estimation of the formation time of a trapped surface by non-local correlation functions

We can also estimate the trapped surface formation time by a characteristic size of the trapped surface [36], i.e.

$$\tau_{therm} \sim \frac{z_b - z_a}{v_z}. \quad (2.43)$$

Here v_z is the velocity of propagation of a signal along the z -direction. We can estimate the velocity of propagation of the signal along the z direction in two ways. We can relate two points on the boundary by the geodesic or the string worldsheet stretched on the static quarks world lines located at these points. The geodesic as well as the worldsheet have maximum z -coordinates, z_* . Varying the end points we vary z_* and we can estimate

$$v = \frac{\Delta z_*}{\Delta x} \cdot c, \quad (2.44)$$

here we take into account that any propagation in the x -direction is limited by the light velocity. Below we assume $c = 1$.

Estimation with string. The relation between the interquark distance x and the string maximum holographic coordinate z_m is given by

$$x = 2 \int_0^{z_m} \frac{dz}{\sqrt{\frac{b^4(z)}{b^4(z_m)} - 1}}. \quad (2.45)$$

From this formula we have

$$v = \frac{\Delta z}{\Delta x} = \sqrt{\frac{b^4(z)}{b^4(z_m)} - 1}. \quad (2.46)$$

We see that (2.46) defines the z -dependent velocity. In particular, considering this estimation in the confining background [36, 40] where $1.2 fm < z_m < 1.8 fm$ and we get $\Delta x = \Delta z_m/2.4$. This estimation gives the trapped surface formation time $\tau_{therm} \approx 0.25 fm$.

The estimation with geodesics in the intermediate background gives $\Delta x = \frac{\pi}{2} \Delta z_m$, which is 4 times longer as compared with the string estimation.

3 Thermalization in anisotropic backgrounds

3.1 Setup

3.1.1 Anisotropic metrics

As an anisotropic background (with the space anisotropy) we consider a five-dimensional Lifshitz-like metric [56, 57, 62]

$$ds_{Li}^2 = L^2 \left[\frac{(-dt^2 + dx^2)}{z^2} + \frac{(dy_1^2 + dy_2^2)}{z^{2/\nu}} + \frac{dz^2}{z^2} \right]. \quad (3.1)$$

Let us remind that the anisotropic Lifshitz metric with space symmetry is given by [55, 56, 58–63]

$$ds_{Lif}^2 = L^2 \left[\frac{-dt^2}{z^2} + \frac{(dx^2 + dy_1^2 + dy_2^2)}{z^{2/\nu}} + \frac{dz^2}{z^2} \right]. \quad (3.2)$$

Both metrics for $\nu = 1$ are reduced to the Poincare patch of AdS_5 .

3.1.2 Thermalization due to shock waves collision

This scenario assumes that the main part of multiplicity is produced in an anisotropic regime and this part of multiplicity can be estimated by the trapped surface produced under a collision of the two shock waves in an anisotropic background. This scenario is accepted in the recent paper [38], where collisions of shock waves in the Lifshitz-like background have been considered.

As a model of anisotropic background we consider a five-dimensional Lifshitz-like metric (3.1). The shock domain wall moving in the v -direction is given by deformation of the metric (3.1)

$$ds_{DW,Ll}^2 = ds_{Ll}^2 + L^2 \frac{\phi(z)\delta(u)}{z^2} du^2, \quad (3.3)$$

with the profile function $\phi(z)$ satisfying

$$\frac{\partial^2 \phi(z)}{\partial z^2} - \left(1 + \frac{2}{\nu}\right) \frac{1}{z} \frac{\partial \phi(z)}{\partial z} = -16\pi G_5 J_{uu}, \quad J_{uu} = E \left(\frac{z}{L}\right)^{1+2/\nu} \delta(z - z_*), \quad (3.4)$$

where z_* is the z -coordinate of the collision point. The entropy can be written in terms of z_a and z_b defining the location of the trapped surface

$$s = \frac{\nu}{4G_5} \left(\frac{1}{(z_a)^{2/\nu}} - \frac{1}{(z_b)^{2/\nu}} \right). \quad (3.5)$$

The analog of relation (2.15) is

$$z_a^{-1-2/\nu} + z_b^{-1-2/\nu} = \frac{8\pi G_5 E}{L^{2/\nu+3}}. \quad (3.6)$$

The maximal entropy is achieved at $z_b \rightarrow \infty$ and it is

$$s = \frac{\nu}{4G_5} (8\pi G_5)^{2/(\nu+2)} E^{2/(\nu+2)}. \quad (3.7)$$

The leading asymptotic gives rise to the value of multiplicity, which is the most compatible to the experimental data, for $\nu = 4$ [38]. Note, that as in the isotropic case for intermediate values of the energy we have to take into account the next to leading term, but now we do not have a restriction on z_a from below since we do not obliged to fit our metric to the metric with a given b -factor. We have changed the background on which we consider the collisions of domain walls. It would be interesting to find "top-down" motivations for consideration the anisotropic background as a holographic model for HIC.

3.2 Thermalization time in the anisotropic background

3.2.1 Estimation with Vaidya metric

We can estimate the thermalization time in the anisotropic background

$$ds^2 = b^2(z) \left(-\frac{f(z_h, z)}{z^{2(\nu-1)}} dv^2 - 2\frac{dv dz}{z^{\nu-1}} + d\vec{x}^2 \right), \quad (3.8)$$

$$f(z_h, z) = 1 - \frac{K(z)}{K(z_a)}. \quad (3.9)$$

For metric (3.8) with $f(z_h, z)$ as in (3.9) we have

$$\ell = 2s \int_0^1 \frac{b(s)}{b(sw)} \frac{dw}{\sqrt{\left(1 - \frac{K(sw)}{K(z_a)}\right) \cdot \left(1 - \frac{b^2(s)}{b^2(sw)}\right)}}, \quad (3.10)$$

$$\tau = s^\nu \int_0^1 \frac{dw}{w^{1-\nu} \left(1 - \frac{K(sw)}{K(z_a)}\right)}. \quad (3.11)$$

For the power-law b -factor, $b(z) = (L/z)^a$ the blackening factor is given by (3.9) with

$$K(z) = z^{ad+\nu} \quad (3.12)$$

Thermalization for these models have been considered in [51, 52]. In Fig.7 we show the dependence of the thermalization time on the distance for the model with $a = 0.5$ and different z_h . We see that increasing the anisotropy the dependence on the horizon position increases as well. We also see that the breaking of the geodesics appears at smaller distances for the case of small z_h (heavy black masses).

For the confining b -factor by the analogy with (2.24) we use the "phenomenological" blackening function

$$K(z) = z^{3+\nu}. \quad (3.13)$$

In Fig.9 the influence of the anisotropy on the thermalization time for the confining metric (3.8) for different c is presented. We see that anisotropy essentially decreases the thermalization time. Meanwhile there is no essential dependence of the thermalization time on the mass of the shell.

3.2.2 Estimation with non-local correlation functions

To estimate the trapped surface formation time we use an analog of estimations (2.43) and (2.44). Considering the relation between the interquark distance along y_1 -direction

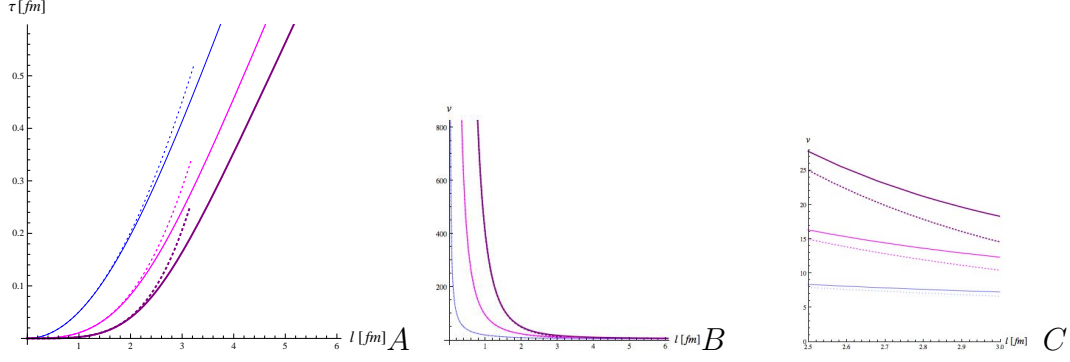


Figure 7. A. Dependencies of t on l for 5-dimensional case for $a = 0.5$ and different ν and different z_h : solid lines $z_h = 1$ and dotted lines $z_h = 2$. Blue lines: $\nu = 2$; magenta lines: $\nu = 3$; purple lines: $\nu = 4$. B. Dependencies of velocity of thermalization propagation on the distance. The zoom to the plot B.

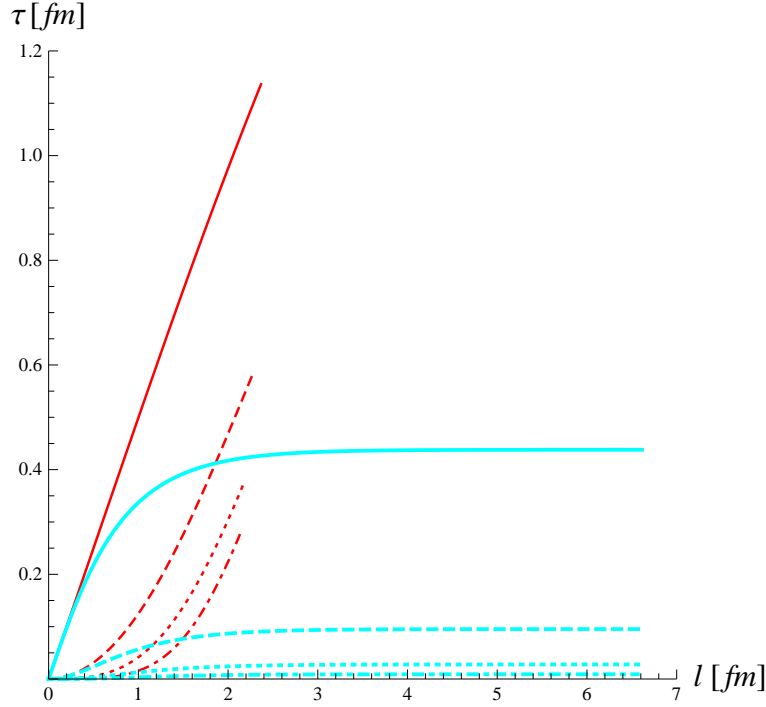


Figure 8. Dependencies of τ on ℓ for the 5-dimensional metric (3.8) and the blackening factor (3.13) for different values of c and ν . Red lines correspond to the AdS case, $c = 0$ and cyan lines to the confining b-factor with $c = 2.56 fm^{-2}$. The isotropic case, $\nu = 1$, is shown by solid lines, anisotropic cases with $\nu = 2$ are shown by dashed lines, $\nu = 3$ by dotted lines and $\nu = 4$ by dot-dashed lines. For all cases $z_a = 1.2 fm$.

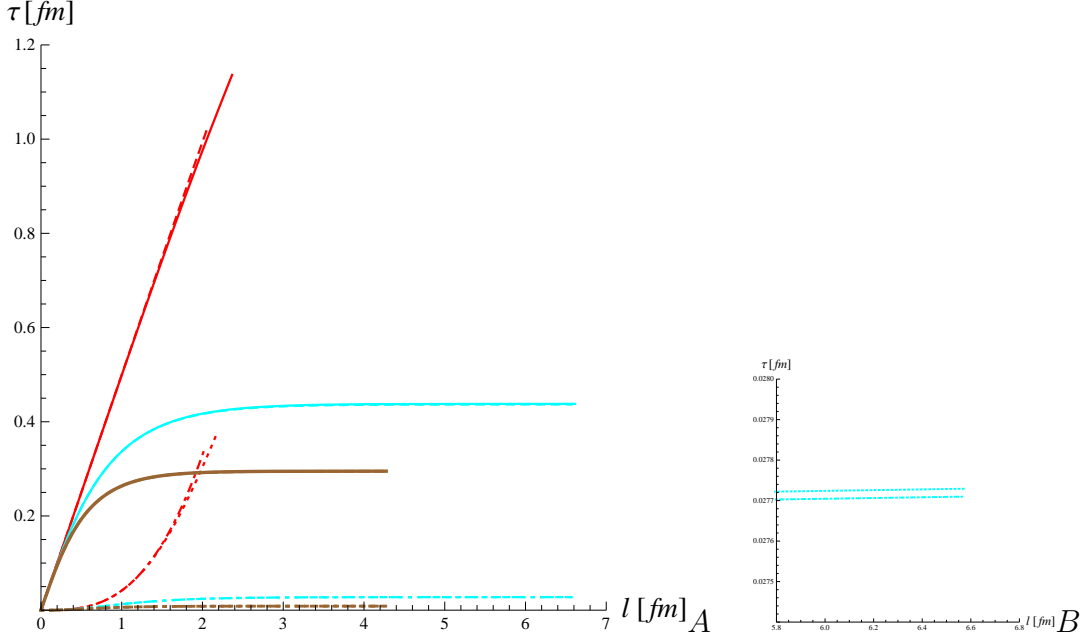


Figure 9. Dependencies of τ on ℓ for 5-dimensional metric (3.8) and blackening factor (3.13) for different c , different ν and different z_a . Red lines correspond to the AdS case, $c = 0$: isotropic case ($\nu = 1$) solid $z_a = 1.2$ and $z_a = 1.8$ dashed lines, anisotropic case ($\nu = 3$) $z_a = 1.2$ dotted and $z_a = 1.8$ dot-dashed lines. Cyan lines correspond to the confining b -factor with $c = 2.65$: isotropic case ($\nu = 1$) $z_a = 1.2$ solid and $z_a = 1.8$ dashed lines, anisotropic case ($\nu = 3$) $z_a = 1.2$ dotted and $z_a = 1.8$ dot-dashed lines. Brown lines correspond to the confining b -factor with $c = 5.75$ and different anisotropy factors and different z_a : isotropic case $z_a = 1.2$ solid and $z_a = 1.8$ dashed lines, anisotropic case ($\nu = 3$) $z_a = 1.2$ dotted and $z_a = 1.8$ dot-dashed lines. B. The zoom of plot A, $5.8 \text{ fm} < \ell < 6.8 \text{ fm}$, $0.027 \text{ fm} < \tau < 0.028 \text{ fm}$.

and the maximum of the string profile holographic coordinate z_m we get the relation

$$y_1 = 2z_m^{1/\nu} \int_0^1 \frac{dy}{\sqrt{1 - z^{2-2/\nu}}}. \quad (3.14)$$

In particular for $\nu = 4$ we have $y_1 = 2.22 z_m^{1/4}$ and therefore, $\Delta y \approx 0.55 \frac{\Delta(z_m)}{z_m^{3/4}}$, that for the trapped surface located at the intermediate zone $1.3 \text{ fm} < z < 1.8 \text{ fm}$ gives $\tau_{\text{therm}} \approx 0.2 \text{ fm}/c$.

Note, that the estimation with geodesics, gives $y_1 = 2\nu z_m^{1/\nu}$, which is once again in four times longer as compared with the string estimation.

One can compare these estimations of the trapped surface formation time with the thermalization time at scale about $2 \text{ fm} \div 4 \text{ fm}$, that is according sect. 3.2.1 for $\nu = 4$ is $\sim 0.05 \text{ fm}$.

4 Conclusion

As it has been mentioned in the Introduction, the entropy of the black hole produced in the shock wave collision predicts multiplicities for heavy ion collisions at RHIC and LHC only for special backgrounds. In this paper we have estimated the thermalization time for these cases.

In particular, we have estimated the anisotropic thermalization time in a holographic bottom-up AdS/QCD confinement backgrounds that provides the Cornell potential and QCD β -function. We have shown that thermalization time is up to 5 times faster comparing to the isotropic case. It is interesting that we have not seen essential dependence of the thermalization time on the temperature, i.e. our method predicts the same order of anisotropic thermalization time for RHIC and LHC.

Acknowledgments

This work is supported by the Russian Science Foundation (project 14-50-00005, Steklov Mathematical Institute). The author is grateful Dmitrii Ageev, Anastasia Golubtsova and Igor Volovich for useful discussions.

References

- [1] J. M. Maldacena, “The Large N limit of superconformal field theories and supergravity,” *Adv. Theor. Math. Phys.* **2**, 231-252 (1998), [hep-th/9711200].
- [2] S. S. Gubser, I. R. Klebanov, A. M. Polyakov, “Gauge theory correlators from noncritical string theory,” *Phys. Lett.* **B428**, 105-114 (1998), [hep-th/9802109].
- [3] E. Witten, “Anti-de Sitter space and holography,” *Adv. Theor. Math. Phys.* **2**, 253-291 (1998), [hep-th/9802150].
- [4] J. Casalderrey-Solana, H. Liu, D. Mateos, K. Rajagopal, U. A. Wiedemann, “Gauge/String Duality, Hot QCD and Heavy Ion Collisions,” [arXiv:1101.0618 [hep-th]].
- [5] I. Ya. Aref’eva, “Holographic approach to quark-gluon plasma in heavy ion collisions,” *Phys. Usp.* **57**, 527 (2014).
- [6] O. DeWolfe, S. S. Gubser, C. Rosen and D. Teaney, “Heavy ions and string theory,” *Prog. Part. Nucl. Phys.* **75**, 86 (2014), [arXiv:1304.7794 [hep-th]].
- [7] J. Polchinski and M. J. Strassler, “The String dual of a confining four-dimensional gauge theory,” hep-th/0003136.

- [8] J. Polchinski and M. J. Strassler, “Deep inelastic scattering and gauge / string duality,” JHEP **0305**, 012 (2003) [hep-th/0209211];
- [9] J. Babington, J. Erdmenger, N. J. Evans, Z. Guralnik and I. Kirsch, “Chiral symmetry breaking and pions in non-supersymmetric gauge/gravity duals,” Phys. Rev. D **69**, 066007 (2004), [arXiv:hep-th/0306018].
- [10] M. Kruczenski, D. Mateos, R. C. Myers and D. J. Winters, “Towards a holographic dual of large N(c) QCD,” JHEP **0405**, 041 (2004), [hep-th/0311270].
- [11] T. Sakai and S. Sugimoto, “Low energy hadron physics in holographic QCD,” Prog. Theor. Phys. **113**, 843 (2005); [arXiv:hep-th/0412141]. T. Sakai and S. Sugimoto, “More on a holographic dual of QCD,” Prog. Theor. Phys. **114**, 1083 (2006). [arXiv:hep-th/0507073].
- [12] J. Erlich, E. Katz, D. T. Son and M. A. Stephanov, “QCD and a holographic model of hadrons,” Phys. Rev. Lett. **95**, 261602 (2005). [arXiv:hep-ph/0501128].
- [13] A. Karch, E. Katz, D. T. Son and M. A. Stephanov, “Linear confinement and AdS/QCD,” Phys. Rev. D **74**, 015005 (2006).
- [14] O. Andreev and V. I. Zakharov, “Heavy-quark potentials and AdS/QCD,” Phys. Rev. D **74**, 025023 (2006), [hep-ph/0604204].
- [15] O. Andreev and V. I. Zakharov, “The Spatial String Tension, Thermal Phase Transition, and AdS/QCD,” Phys. Lett. B **645**, 437 (2007), [hep-ph/0607026]. [hep-ph/0607026]
- [16] C. D. White, “The Cornell potential from general geometries in AdS / QCD,” Phys. Lett. B **652**, 79 (2007), [hep-ph/0701157].
- [17] H. J. Pirner and B. Galow, “Strong Equivalence of the AdS-Metric and the QCD Running Coupling,” Phys. Lett. B **679**, 51 (2009), [arXiv:0903.2701 [hep-ph]].
- [18] B. Galow, E. Megias, J. Nian and H. J. Pirner, “Phenomenology of AdS/QCD and Its Gravity Dual,” Nucl. Phys. B **834**, 330 (2010), [arXiv:0911.0627 [hep-ph]].
- [19] S. He, M. Huang and Q. -S. Yan, “Logarithmic correction in the deformed AdS₅ model to produce the heavy quark potential and QCD beta function,” Phys. Rev. D **83**, 045034 (2011), [arXiv:1004.1880 [hep-ph]].
- [20] U. Gursoy, E. Kiritsis, L. Mazzanti and F. Nitti, “Holography and Thermodynamics of 5D Dilaton-gravity,” JHEP **0905**, 033 (2009), [arXiv:0812.0792 [hep-th]].
- [21] U. Gursoy, E. Kiritsis, L. Mazzanti, G. Michalogiorgakis and F. Nitti, “Improved Holographic QCD,” Lect. Notes Phys. **828**, 79 (2011), [arXiv:1006.5461 [hep-th]].
- [22] P. M. Chesler and W. van der Schee, “Early thermalization, hydrodynamics and energy loss in AdS/CFT,” arXiv:1501.04952 [nucl-th].

- [23] S. S. Gubser, S. S. Pufu and A. Yarom, “Entropy production in collisions of gravitational shock waves and of heavy ions,” *Phys. Rev. D* **78**, 066014 (2008), [arXiv:0805.1551 [hep-th]].
- [24] J. L. Albacete, Y. V. Kovchegov and A. Taliotis, “Modeling Heavy Ion Collisions in AdS/CFT,” *JHEP* **0807**, 100 (2008), [arXiv:0805.2927 [hep-th]].
- [25] L. Alvarez-Gaume, C. Gomez, A. Sabio Vera, A. Tavanfar and M. A. Vazquez-Mozo, “Critical formation of trapped surfaces in the collision of gravitational shock waves,” *JHEP* **0902**, 009 (2009), [arXiv:0811.3969 [hep-th]].
- [26] P. M. Chesler and L. G. Yaffe, “Horizon formation and far-from-equilibrium isotropization in supersymmetric Yang-Mills plasma,” *Phys. Rev. Lett.* **102**, 211601 (2009), [arXiv:0812.2053 [hep-th]].
- [27] S. Lin and E. Shuryak, “Grazing Collisions of Gravitational Shock Waves and Entropy Production in Heavy Ion Collision,” *Phys. Rev. D* **79**, 124015 (2009), [arXiv:0902.1508 [hep-th]].
- [28] S. S. Gubser, S. S. Pufu and A. Yarom, “Off-center collisions in AdS(5) with applications to multiplicity estimates in heavy-ion collisions,” *JHEP* **0911**, 050 (2009), [arXiv:0902.4062 [hep-th]].
- [29] I. Ya. Aref’eva, A. A. Bagrov and E. A. Guseva, “Critical Formation of Trapped Surfaces in the Collision of Non-expanding Gravitational Shock Waves in de Sitter Space-Time,” *JHEP* **0912**, 009 (2009); [arXiv:0905.1087 [hep-th]]. I. Ya. Aref’eva, A. A. Bagrov and L. V. Joukovskaya, “Critical Trapped Surfaces Formation in the Collision of Ultrarelativistic Charges in (A)dS,” *JHEP* **1003**, 002 (2010), [arXiv:0909.1294 [hep-th]].
- [30] S. Lin and E. Shuryak, “On the critical condition in gravitational shock wave collision and heavy ion collisions,” *Phys. Rev. D* **83**, 045025 (2011) [arXiv:1011.1918 [hep-th]].
- [31] I. Ya. Aref’eva, A. A. Bagrov and E. O. Pozdeeva, “Holographic phase diagram of quark-gluon plasma formed in heavy-ions collisions,” *JHEP* **1205**, 117 (2012) [arXiv:1201.6542 [hep-th]].
- [32] E. Kiritsis and A. Taliotis, “Multiplicities from black-hole formation in heavy-ion collisions,” *JHEP* **1204**, 065 (2012); [arXiv:1111.1931 [hep-ph]]. A. Taliotis, “Extra dimensions, black holes and fireballs at the LHC,” *JHEP* **1305**, 034 (2013), [arXiv:1212.0528 [hep-th]].
- [33] I. Ya. Aref’eva, E. O. Pozdeeva and T. O. Pozdeeva, “Holographic estimation of multiplicity and membranes collision in modified spaces AdS_5 ,” *Theor. Math. Phys.* **176**, 861 (2013); [arXiv:1401.1180 [hep-th]].
- [34] I. Ya. Aref’eva, E. O. Pozdeeva and T. O. Pozdeeva, “Holographic estimation of

- multiplicity and membranes collision in modified spaces AdS_5 ,” arXiv:1401.1180 [hep-th]; “Potentials in modified AdS_5 spaces with a moderate increase in entropy,” Theor. Math. Phys. **180**, 781 (2014)
- [35] G. Aad *et al.* [ATLAS Collaboration], “Measurement of the centrality dependence of the charged particle pseudorapidity distribution in lead-lead collisions at $\sqrt{s_{NN}} = 2.76$ TeV with the ATLAS Phys. Lett. B **710**, 363 (2012), [arXiv:1108.6027 [hep-ex]].
- [36] D. S. Ageev and I. Ya. Aref’eva, “Holographic Thermalization in Quark Confining Background,” ZhETP, 147 **180**, 1 (2015), arXiv:1409.7558 [hep-th].
- [37] M. Strickland, “Thermalization and isotropization in heavy-ion collisions,” arXiv:1312.2285 [hep-ph].
- [38] I. Ya. Aref’eva and A. A. Golubtsova, “Shock waves in Lifshitz-like spacetimes,” arXiv:1410.4595 [hep-th].
- [39] D. Giataganas, “Observables in Strongly Coupled Anisotropic Theories,” PoS Corfu **2012**, 122 (2013), [arXiv:1306.1404 [hep-th]].
- [40] I. Ya. Aref’eva, *Holographic description of thermalization in heavy ion collisions*, to appear in the proceedings of the conference ‘Quark Confinement and the Hadron Spectrum XI’, St. Petersburg, September 8-12 2014
- [41] U. H. Danielsson, E. Keski-Vakkuri and M. Kruczenski, “Spherically collapsing matter in AdS, holography, and shellons,” Nucl. Phys. B **563**, 279 (1999). [arXiv:hep-th/9905227].
- [42] J. Abajo-Arrastia, J. Aparicio and E. Lopez, “Holographic Evolution of Entanglement Entropy,” JHEP 1011, 149 (2010), arXiv:1006.4090 [hep-th]
- [43] V. Balasubramanian, A. Bernamonti, J. de Boer, N. Copland, B. Craps, E. Keski-Vakkuri, B. Muller and A. Schafer *et al.*, “Thermalization of Strongly Coupled Field Theories,” Phys. Rev. Lett. **106** (2011) 191601, [arXiv:1012.4753 [hep-th]].
- [44] V. Balasubramanian, A. Bernamonti, J. de Boer, N. Copland, B. Craps, E. Keski-Vakkuri, B. Muller and A. Schafer *et al.*, “Holographic Thermalization,” Phys. Rev. D **84** (2011) 026010, [arXiv:1103.2683 [hep-th]].
- [45] J. Aparicio and E. Lopez, “Evolution of Two-Point Functions from Holography,” JHEP **1112**, 082 (2011), [arXiv:1109.3571 [hep-th]].
- [46] R. Callan, J. -Y. He and M. Headrick, “Strong subadditivity and the covariant holographic entanglement entropy formula,” JHEP **1206**, 081 (2012), arXiv:1204.2309.
- [47] D. Galante and M. Schvellinger, “Thermalization with a chemical potential from AdS spaces,” JHEP **1207**, 096 (2012), [arXiv:1205.1548 [hep-th]].

- [48] E. Caceres and A. Kundu, “Holographic Thermalization with Chemical Potential,” JHEP **1209**, 055 (2012) [arXiv:1205.2354 [hep-th]].
- [49] I. Ya. Arefeva and I. V. Volovich, “On Holographic Thermalization and Dethermalization of Quark-Gluon Plasma,” Theor. Math. Phys. **174**, 186 (2013), arXiv:1211.6041 [hep-th].
- [50] I. Aref’eva, A. Bagrov and A. S. Koshelev, “Holographic Thermalization from Kerr-AdS,” JHEP **1307**, 170 (2013), [arXiv:1305.3267 [hep-th]].
- [51] V. Keranen, E. Keski-Vakkuri and L. Thorlacius, “Thermalization and entanglement following a non-relativistic holographic quench,” Phys. Rev. D **85**, 026005 (2012), [arXiv:1110.5035 [hep-th]].
- [52] M. Alishahiha, E. O Colgain and H. Yavartanoo, “Charged Black Branes with Hyperscaling Violating Factor,” JHEP **1211**, 137 (2012), [arXiv:1209.3946 [hep-th]].
- [53] M. Alishahiha, A. F. Astaneh and M. R. M. Mozaffar, “Thermalization in backgrounds with hyperscaling violating factor,” Phys. Rev. D **90**, no. 4, 046004 (2014) [arXiv:1401.2807 [hep-th]].
- [54] P. Fonda, L. Franti, V. Keranen, E. Keski-Vakkuri, L. Thorlacius and E. Tonni, “Holographic thermalization with Lifshitz scaling and hyperscaling violation,” arXiv:1401.6088 [hep-th].
- [55] S. Kachru, X. Liu and M. Mulligan, Gravity duals of Lifshitz-like Fixed points, Phys.Rev. D78 (2008) 106005; [arXiv:0808.1725].
- [56] M. Taylor, “Non-relativistic holography,” [arXiv:0812.0530 [hep-th]].
- [57] S.S. Pal, Anisotropic gravity solutions in AdS/CMT, [arXiv:0901.0599]
- [58] J. Tarrio, S. Vandoren, “Black holes and black branes in Lifshitz spacetimes,” JHEP **1109**, 017 (2011). [arXiv:1105.6335 [hep-th]].
- [59] B. Gouteraux and E. Kiritsis, “Generalized Holographic Quantum Criticality at Finite Density,” JHEP **1112**, 036 (2011) [arXiv:1107.2116 [hep-th]].
- [60] L. Huijse, S. Sachdev and B. Swingle, “Hidden Fermi surfaces in compressible states of gauge-gravity duality,” Phys. Rev. B **85**, 035121 (2012) [arXiv:1112.0573 [cond-mat.str-el]].
- [61] X. Dong, S. Harrison, S. Kachru, G. Torroba and H. Wang, “Aspects of holography for theories with hyperscaling violation,” JHEP **1206**, 041 (2012) [arXiv:1201.1905 [hep-th]].
- [62] P. Bueno, W. Chemissany, P. Meessen, T. Ortin and C. S. Shahbazi, “Lifshitz-like Solutions with Hyperscaling Violation in Ungauged Supergravity,” JHEP **1301**, 189 (2013) [arXiv:1209.4047 [hep-th]].

- [63] B. Gouteraux and E. Kiritsis, “Quantum critical lines in holographic phases with (un)broken symmetry,” JHEP **1304**, 053 (2013) [arXiv:1212.2625 [hep-th]].